

Creating Aligned, Elongated Pores in Titanium Foams by Swaging of Preforms with Ductile Space-Holder**

By Yasumasa Chino* and David C. Dunand

The low density, high strength, and excellent chemical resistance of titanium make titanium foams an attractive choice for structural applications,^[1] e.g., as cores in sandwiches for load-bearing structures^[2] or for porous bone-replacement implants.^[3–4] Few reports describe titanium foams with aligned, elongated pores, which are of particular interest for biomedical implants as they mimic the anisotropic porous architecture of bone which is responsible for its structural and mechanical anisotropic properties.^[5]

One method for creating aligned, elongated pore in titanium is the lotus-metal technique, where titanium is unidirectionally solidified in a hydrogen/argon atmosphere.^[6] Due to titanium's high melting point and extreme susceptibility for contamination, all other methods for creating aligned, elongated pores in titanium rely on powder metallurgy, such as pressurized pore expansion method,^[7–9] utilization of unidirectional freeze-casting,^[10] and utilization of solid space-holders.^[11–12]

Here, we focus on the fugitive space-holder method which to date has only been demonstrated once for titanium: Tuchinskiy and Loutfy^[12] extruded rods, consisting of a fugitive core and a shell made of titanium powders and polymer binder, cut the rods into segments, poured the segments into a die and compressed them to produce a green composite. Binder and filler thermal removal followed by sintering resulted in a titanium foam with short, randomly oriented elongated pores. The authors point to the challenge of identifying filler and binder which do not result in titanium contamination, but they neither disclose the composition of their filler/binder nor present data on foam contamination. Increases in carbon and/or oxygen content in titanium lead to a steady reduction in tensile ductility up to a carbon or oxygen contents of ~0.5 wt% where titanium becomes brittle in tension.^[13]

Recently, Weil *et al.*^[14,15] developed a new powder injection molding (PIM) binder system, where naphthalene (C₁₀H₈) is

used as a binder to produce full-density titanium parts by sintering: the high vapor pressure of naphthalene allows its complete removal by vacuum sublimation before sintering, thus reducing carbon contamination of the sintered titanium product. Weil *et al.*^[16] further demonstrated that equiaxed porosity in the range of 7–32 vol% could be created in titanium by increasing the amount of naphthalene.

Here, we use naphthalene as a fugitive space-holder in titanium powder preforms for the same reasons advanced by Weil *et al.*^[14–16] Additionally, we choose naphthalene because it shows rapid creep at room temperature,^[17] so that the room-temperature swaging of a preform of titanium powders with naphthalene inclusions is expected to align and elongate these inclusions into an ellipsoidal shape which, after sublimation, result in aligned, elongated pores in the titanium preform and the subsequent sintered foam.

The fabrication procedure is outlined in Figure 1. We use unalloyed titanium powders with particle sizes < 40 μm (from Aremco, Atlantic Equipment Engineering, NJ) showing irregular shapes typical of the hydride–dehydride process. The organic components are the same as those used by Weil *et al.*^[16] and consist of 93 vol% naphthalene (Aldrich Chemical Co., MO) as fugitive space-holder, 6 vol% EVA (Poly(ethylene-co-vinyl acetate), Aldrich Chemical Co.) as binder and 1 vol% stearic acid (Aldrich Chemical Co.) as powder surfactant. The titanium powders and organic components, with 40:60 volume ratio (73:27 mass ratio), are mixed thoroughly at 100 °C, where naphthalene and EVA are melted and coat the titanium powders, and then solidified. The solidified mixture is then crushed in a mortar to eliminate agglomerates, and packed in a low carbon steel (AISI 1010) tube with inner diameter, outer diameter, and length of 7.0, 9.7, and 130 mm, respectively.

The tube is brought to 60 °C by heating in a furnace for 20 min and swaged multiple times at that temperature (which is well below the 80 °C melting point of naphthalene) at a cross-section reduction ratio of 32% (for the first two passes) and 14% (for the following passes). The tube is re-heated to 60 °C between each swaging pass and is not completely sealed so air within the tube can be released during the swaging passes. Three tubes were swaged for 3, 5, and 6 passes, corresponding to equivalent strains of 0.65, 0.89, and 1.1, respectively, calculated as $\epsilon_{eq} = 2\ln(d/d_0)$ where d and d_0 are the final and initial diameters of the tube, respectively.^[18] The tubes are then cut into 20 mm segments, and heated at 73 °C for 9 h under a dynamic vacuum of 1 kPa to sublimate the naphthalene (which displays a vapor pressure of 1 kPa at its

[*] Dr. Y. Chino

Materials Research Institute for Sustainable Development,
National Institute of Advanced Industrial Science and
Technology

Nagoya, 463-8560, Japan

E-mail: y-chino@aist.go.jp

Prof. D. C. Dunand

Department of Materials Science and Engineering, North-
western University, Evanston, Illinois, 60208, USA

[**] This research was supported by the US National Science
Foundation through grant DMR-0505772.

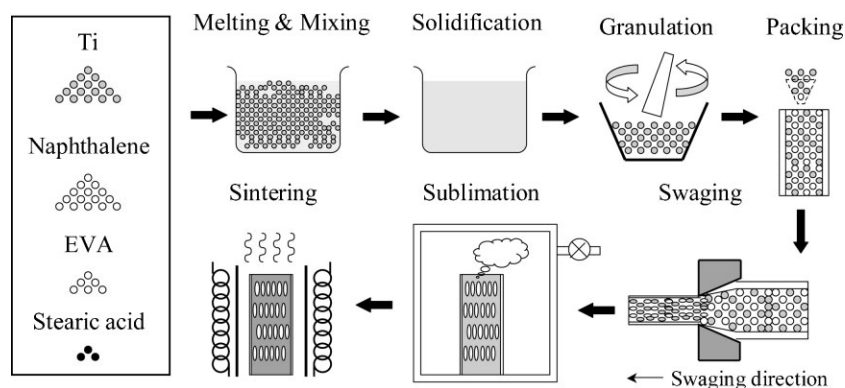


Fig. 1. Schematic of process used to create titanium foams with aligned, elongated pores.

melting point of 80 °C).^[19] The mass of a swaged segment was found to decrease steadily with sublimation time until reaching a constant value after ~9 h., indicating that all naphthalene has been sublimed. The resulting porous titanium preform within its tube is then pre-sintered under a high vacuum of 10^{-2} Pa at 300 °C for 3 h and finally sintered under 10^{-3} Pa at 1070 °C for 2 h. The sintered samples are removed from the tube by electro-discharge machining.

Metallographic examination of the sintered samples is performed by scanning electron microscopy (SEM) on ground and polished samples whose porosity is filled with epoxy, as shown in Figure 2 and 3, for longitudinal cross-section of the three foams with different preform reduction ratios. These

micrographs reveal that there are two types of pores in the foams: a) small pores, less than $\sim 40 \mu\text{m}$ in apparent equivalent diameter (defined a spherical pore with the same volume as the real pore), present between titanium powders as a result of incomplete sintering of the powders; and b) large pores, more than $\sim 100 \mu\text{m}$ in apparent equivalent diameter, originating from sublimated naphthalene-based inclusions (and possibly air pockets entrapped between the naphthalene inclusions). The shape of the small pores remains roughly equiaxed independently of the equivalent strain, suggesting that no plastic deformation of titanium powders is occurring during swaging, as expected given the low temperature used. These pores could

be reduced by sintering to temperatures higher than used here. For the large pores, higher equivalent strain results in microstructure showing longer and more aligned pores along the swaging direction, as expected if they replicate naphthalene-based inclusions that were elongated by plastic deformation during swaging. These pores are expected to be interconnected into a complex three-dimensional network (not apparent in these cross-sections) given that the naphthalene-based space-holder was removed by sublimation from the preform.

The apparent density of the sintered samples is measured by the Archimedes method in deionized water, after coating with a thin layer of vacuum grease to prevent water penetration in open pores, thus yielding direct measurement of the total porosity. Total porosity of the foams with different equivalent strains ($\epsilon_{eq} = 0.65, 0.89, \text{ and } 1.1$) is 61, 65, and 49%, respectively. The decrease in porosity for the foam with the highest strain in the preform is likely related to the improved packing, removal of entrapped air and possibly partial cold densification of the titanium powders in the preform by swaging.

Figure 4a shows the evolution, with increasing preform equivalent strain, in the pore length and width in the cross-sections, as measured for large pore (with equivalent diameter $> 50 \mu\text{m}$) by image analysis with the commercially available software Image-Pro Plus. The large error range reflecting the bimodal size distribution of pores weakens the expected trend of increasing pore length and decreasing pore width with increasing equivalent strain, which is however qualitatively apparent when examining micrographs (Fig. 2a–c). Aspect ratios were also measured for large pores (with equivalent diameter $> 50 \mu\text{m}$), and average values are shown in Fig. 4b. While the error bars are large too, it is

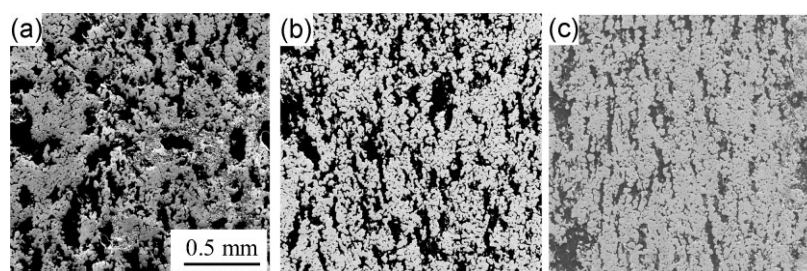


Fig. 2. SEM micrographs showing longitudinal cross-sections of titanium foams with various preform equivalent strains: (a) $\epsilon_{eq} = 0.65$, (b) $\epsilon_{eq} = 0.89$, and (c) $\epsilon_{eq} = 1.1$. Pores replicating naphthalene-based inclusions become more elongated and aligned with the swaging direction (arrow) as ϵ_{eq} increases.

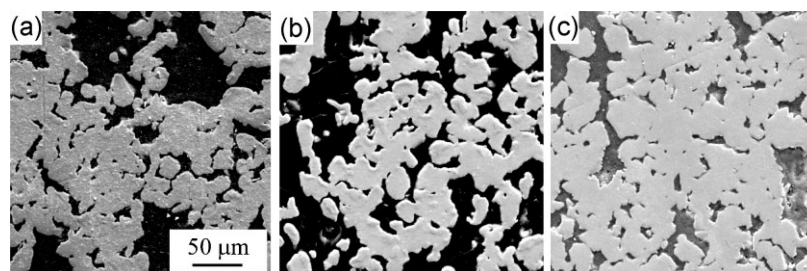


Fig. 3. Higher magnification SEM micrographs of titanium foams shown in Fig. 2: (a) $\epsilon_{eq} = 0.65$, (b) $\epsilon_{eq} = 0.89$, and (c) $\epsilon_{eq} = 1.1$, with swaging direction given by arrow. Small, equiaxed pores resulting from incomplete sintering of powders and larger, elongated pores replicating naphthalene-based inclusions are visible.

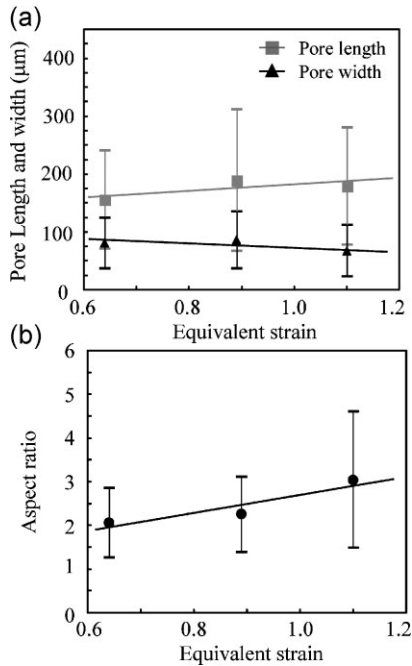


Fig. 4. (a) Plot of titanium foam pore length and width versus preform equivalent strain; (b) Plot of aspect ratio of large pores versus preform equivalent strain.

apparent that the aspect ratio of the large pores increases with increasing equivalent strain, reaching an average value of 3.0 (and a maximum value of 8.3) for the largest preform strain of $\epsilon_{eq} = 1.1$. These values are comparable to the average aspect ratios of elongated pores in foams processed by the pressurized pore expansion method (~ 2),^[7,9] but inferior to those of a foam processed by unidirectional freeze casting (> 10).^[10]

Spoerke *et al.*^[7] have investigated the initial in vitro response of primary rat osteoblastic cells to the elongated porous microstructure in titanium foams created by the pressurized pore expansion method, and reported that cell attachment and ingrowth are promoted by the elongated porous microstructure. This indicates that the elongated porous microstructure achieved by the present method may also have the same biological effect, especially if the average size of the large pore is increased from the present value of $\sim 100 \mu\text{m}$ to $150\text{--}200 \mu\text{m}$, which is the ideal pore size for bone ingrowth.^[6] One approach for creating larger pore is to

optimize volume ratio between the titanium powder and organic components.

An important goal associated with the selection as fugitive space-holder of a high vapor pressure compound such as naphthalene is to reduce carbon contamination in the sintered foams. Table 1 lists carbon concentrations of the as-received powders and the foams as measured by ATI Wah Chang (Albany, OR) using the combustion-infrared emission method. The foam carbon concentration shown in Table 1 is an average value of the three foams with three equivalent strains. For comparison, carbon concentrations of porous titanium samples produced by PIM of TiH_2 powders^[14] are also given in Table 1. As expected from the utilization of naphthalene-based space-holder, the carbon concentration of the present foam (0.39 wt%) is successfully maintained below the level ($\sim 0.5 \text{ wt}\%$), where severe embrittlement occurs in pure titanium.^[13] However, the carbon content of the present foams is 2.5–5.2 times higher than that of the sintered titanium-PIM samples.^[14] One possible reason is that the TiH_2 powders are protected from contamination by the subliming naphthalene by their hydrided nature, as demonstrated recently for titanium foams created by gelcasting.^[20] Another likely reason is that the fraction of binder used for the present foams is larger by a factor of 1.2–2.0 as compared to the PIM porous samples. One approach to minimize carbon content in the present foam is to use TiH_2 powders with low carbon levels, which however are more pricy. Another option may be to minimize the quantities of the bonding agent (EVA) which vaporizes less readily than naphthalene.

In summary, titanium foams have been created by swaging titanium powder preforms containing a naphthalene-based fugitive space-holder. Elongated naphthalene-based inclusions resulting from swaging are then sublimated, leaving in the preform elongated pores replicating their shape. Finally, sintering of the titanium preforms results in titanium foams with 49–65 vol% pores consisting of small, roughly equiaxed pores between partially sintered titanium powders and larger, elongated (aspect ratio of 2–3) pores aligned along the swaging direction, from the fugitive space-holder. The carbon content of the sintered foam is 0.39 wt%, which is below the critical level for the occurrence of severe embrittlement in pure titanium.

Received: July 8, 2008

Final version: September 8, 2008

Published online: Dec. 30, 2008

Table 1. Comparison of titanium foams produced by swaging (present work) and porous titanium produced by PIM.^[14] Both use the same naphthalene/EVA/stearic acid mixture as space-holder.

Method	Space holder fraction in preform [vol%]	Metal powder composition and size	Initial carbon content in metal powders [wt%]	Final carbon content after sintering [wt%]	Porosity after sintering [%]
Swaging [Present work]	60	CP Ti ($d < 40 \mu\text{m}$)	0.057	0.39	49–65
PIM [14]	30–50	TiH_2 ($d_{ave} = 8.6 \mu\text{m}$)	0.012	0.075 and 0.145	7–15

-
- [1] D. C. Dunand, *Adv. Eng. Mater.* **2004**, *6*, 369.
- [2] C. F. Li, Z. G. Zhu, *J. Porous Mater.* **2006**, *13*, 21.
- [3] A. Laptev, M. Bram, H. P. Buchkremer, D. Stover, *Powder Metall.* **2004**, *47*, 85.
- [4] N. G. D. Murray, D. C. Dunand, *Compos. Sci. Technol.* **2003**, *63*, 2311.
- [5] S. Weiner, H. D. Wagner, *Annu. Rev. Mater. Sci.* **1998**, *28*, 271.
- [6] Y. Higuchi, Y. Ohashi, H. Nakajima, *Adv. Eng. Mater.* **2006**, *8*, 907.
- [7] E. D. Spoerke, N. G. D. Murray, H. Li, L. C. Brinson, D. C. Dunand, S. I. Stupp, *J. Biomed. Mater. Res.* **2008**, *84A*, 402.
- [8] M. W. Kearns, P. A. Blenkinsop, A. C. Barber, T. W. Farthing, *Int. J. Powder Metall.* **1988**, *24*, 59.
- [9] N. G. Davis, J. Teisen, C. Schuh, D. C. Dunand, *J. Mater. Res.* **2001**, *16*, 1508.
- [10] Y. Chino, D. C. Dunand, *Acta Mater.* **2008**, *56*, 105.
- [11] P. J. Kwok, S. H. Oppenheimer, D. C. Dunand, *Adv. Eng. Mater.* **2008**, *10*, 820.
- [12] L. Tuchinskiy, R. Loutfy, in *Materials and Processes for Medical Devices* (Ed: S. Shrivastava), ASM International, Materials Park (OH) **2003**, p. 1.
- [13] R. I. Jaffee, H. R. Ogden, D. J. Maykuth, *AIME Trans.* **1950**, *188*, 1261.
- [14] E. Nyberg, M. Miller, K. Simmons, K. S. Weil, *Mater. Sci. Eng. C* **2005**, *25*, 336.
- [15] K. S. Weil, E. Nyberg, K. Simmons, *J. Mater. Process. Technol.* **2006**, *176*, 205.
- [16] K. S. Weil, E. A. Nyberg, K. L. Simmons, *Mater. Trans.* **2005**, *46*, 1525.
- [17] V. N. Matveenko, N. V. Pertsov, E. D. Shchukin, *Phys. Status Solidi A* **1980**, *58*, K205.
- [18] G. E. Dieter, *Mechanical Metallurgy*, SI, McGraw-Hill, Singapore **1988**.
- [19] D. R. Lide (Editor in-chief), *CRC Handbook of Chemistry and Physics*, 74th ed., CRC Press Inc, USA **1993**.
- [20] K. A. Erk, D. C. Dunand, K. R. Shull, *Acta Mater.* **2008**, *56*, 5147.
-